DOI: 10.1002/ejic.200601190

Synthesis, Structures and Optical Power Limiting of Some Transition Metal and Lanthanide Monoporphyrinate Complexes Containing Electron-Rich Diphenylamino Substituents

Shitao Fu,[a,b] Xunjin Zhu,[b] Guijiang Zhou,[b] Wai-Yeung Wong,[b] Cheng Ye,[c] Wai-Kwok Wong,*[b] and Zaoying Li*[a]

Keywords: Lanthanides / Optical limiting / Photoluminescence / Porphyrins / Transition metals

Transition metal and lanthanide monoporphyrinate complexes based on 5,10,15,20-tetrakis[*p*-(diphenylamino)-phenyl]-21*H*,23*H*-porphine (H_2tdpapp) have been synthesized and characterized and the X-ray crystal structures of the palladium and platinum analogues [M(tdpapp)] (M = Pd, Pt) determined. Experimental investigations of the nonlinear optical transmittance characteristics at 532 nm show that most of these new metalated porphyrinate complexes are excellent optical limiters with performances comparable or superior to those of the benchmark reverse saturable absorption dyes such as fullerene C_{60} and (phthalocyanine)metal complexes. The nonlinear optical measurements reveal that the optical-limiting effects of porphyrins can be enhanced greatly by incorporation of lanthanide ions and covalent attachment of the electron-donating diphenylamino moieties to the parent porphyrinate ring. The optical-limiting thresholds for these lanthanide monoporphyrinate complexes range from 0.09 to 0.30 J cm^{-2} at 82 % linear transmittance, which makes them attractive candidates as optical-limiting materials for the protection of various optical devices.

Introduction

With the rapid development of laser technology, the damage to human eyes, optical sensors, and optical components caused by exposure to sudden, intense laser pulses has driven the search for effective optical limiters that display fast response speeds and relatively high linear transmissions.[1,2] Optical limiters are materials that are transparent at normal light intensities but opaque to very bright light.[3–5] Over the last decade, interest has focused on materials with weak ground-state absorption and strong excited-state absorption, which typically achieve optical limiting by a mechanism known as reverse saturable absorption (RSA). An ideal material would have a low ground-state absorption over a wide spectral bandwidth and strong excited-state absorption across the same region.[6]

At present, the materials employed for optical power limiting (OPL) are mainly composed of small molecules, such as fullerene (C_{60}),[7,8] phthalocyanines,[9,10] diacetylenes,[11] nanotubes,[12] and organometallic compounds.[13,14] Some conjugated organic polyynes also exhibit good optical-limiting capabilities.[15] Metalloporphyrins are among the most effective optical limiters[6,16–20] because their ground-state absorption is mostly confined to a few narrow regions (Soret and Q-bands), which allows high transmission in the spectral window between these bands. In addition, these macrocycles present a highly developed π-conjugation system which contributes to strong excited-state absorption, high triplet yields, long excited line-like spectra, and long luminescence lifetimes. Porphyrins and metalloporphyrins are known to exhibit RSA at 532 nm. Molecular modifications, for example by incorporating functional groups on the porphyrin ring or inserting metal ions in the ring, are commonly adopted to improve their OPL properties.

Recent investigations on the use of metalloporphyrins for optical limiting have focused on the transition metals,[16] phosphorus(V),[17] and group III and IV metals.[6,18] Wang and co-workers, for example, have reported a series of pentaazadentate porphyrin-like metal complexes with potential uses as optical-limiting materials where the metal ion is Sm^{3+} or Gd^{3+}.[19] A europium(III) tetraphenylporphyrinate complex with OPL capability has also been reported by Kuznetsova et al.[20] It is well known that insertion of the lanthanide ion into the porphyrin core allows the energy of the ligand's triplet state to transfer efficiently to the excited state of the lanthanide ion, thus enabling this ion to emit light.[21] While triarylamine-derived organic materials have been investigated extensively because of their potential applications in various areas of optoelectronic devices,[22] there are only a few reports of porphyrin/triarylamine hybrids.[23] In this paper, we describe the synthesis and charac-

[a] Department of Chemistry, Wuhan University, Wuhan 430072, Hubei, P. R. China
[b] Department of Chemistry and Centre for Advanced Luminescence Materials, Hong Kong Baptist University, Kowloon Tong, Hong Kong, P. R. China
[c] Center for Molecular Sciences, Institute of Chemistry, Chinese Academy of Sciences, Beijing 100080, P. R. China

terization of a series of lanthanide monoporphyrinate complexes [(tdpapp)Ln(L_{OMe})] {Ln = Yb, Er, and Gd; L_{OMe}^- = (η^5-C_5H_5)Co[P(=O)(OMe)$_2$]$^-$, H_2tdpapp = 5,10,15,20-tetrakis[*p*-(diphenylamino)phenyl]-21*H*,23*H*-porphine} and their late transition metal analogues [M(tdpapp)] (M = Ni, Zn, Pd, Pt) which show large optical-limiting capabilities; the mechanisms pertaining to their nonlinear optical behavior are critically discussed.

Results and Discussion

Synthesis and Characterization

Scheme 1 shows the chemical structures and the synthetic strategies of the metal monoporphyrinate complexes discussed in the present study. The porphyrin free-base (H_2tdpapp) containing diphenylamino (DPA) units was prepared according to a literature procedure.[24] When the molar ratio of pyrrole/DDQ (DDQ = 2,3-dichloro-5,6-dicyano-1,4-benzoquinone) was set at 4:3, the synthetic yield improved by up to 52%. The precursor complex Ln[N(SiMe$_3$)$_2$]$_3$·*x*[LiCl(thf)$_3$] (Ln = Yb, Er, and Gd) was generated from the reaction of anhydrous $LnCl_3$ with 3 equiv. of Li[N(SiMe$_3$)$_2$] in thf. An excess of the precursor complex was treated with the porphyrin free-base under nitrogen, and the mixture was refluxed in toluene for 12 h. Excess NaL_{OMe} was then added to the reaction mixture at room temperature. This procedure gave green crystals of [(tdpapp)Ln(L_{OMe})] [Ln = Yb (**1**), Er (**2**), Gd (**3**)] in about 80% yield. These lanthanide complexes are thermally and air-stable, and could be purified by column chromatography, which indicates that the tripodal anion is capable of stabilizing labile normal lanthanide(III) porphyrinate complexes by effectively encapsulating the lanthanide(III) ion and thereby shielding it from interactions with the environment. The transition metal porphyrinate complexes [M(tdpapp)] [M = Ni (**4**), Zn (**5**), Pd (**6**), Pt (**7**)] were synthesized by refluxing the porphyrin free-base with 1 equiv. of the metal salts in an appropriate solvent. Purification was effected by preparative thin layer chromatography (TLC) with high isolated yields of 87–96%. All of these metal monoporphyrinate complexes were characterized by accurate mass spectrometric and spectroscopic techniques. The electrospray ionization high-resolution (ESI-HR) mass spectra of **1**–**3** exhibit the $[M + 1]^+$ or $[M]^+$ peak at *m*/*z* = 1906.4548, 1899.4461, and 1890.4455, respectively, which deviate by less than 5 ppm from the theoretical values of 1906.4627, 1899.4488, and 1890.2683; their isotopic distribution patterns match the theoretical fittings very well. The ^{31}P NMR spectra (vs. 85% H_3PO_4) of **1** and **2** display a single peak at δ = 68.29 and –166.01 ppm, respectively.

The solid-state structures of complexes **6** and **7** were also confirmed by X-ray crystallographic studies. Perspective drawings of **6** and **7** are displayed in Figure 1, and Table 1 lists selected bond lengths and angles. There is only half of the molecule per asymmetric unit in the unit cell in each case, and the porphyrin framework is essentially planar. The group 10 metal ion is coordinated to the four pyrrolic nitrogen atoms, as is typical of other normal metalated porphyrinates. The bond lengths and angles in the porphyrin ring are also similar to those observed in the 5,10,15,20-tetraarylporphyrin system.[25,26]

The absorption spectra of all the new complexes were also measured and, in general, show a bathochromic shift in the absorption features after adding the diphenylamino chromophores (see Exp. Sect.). For example, complexes **1**–**3** show typical Soret and Q-bands for the lanthanide monoporphyrinate complexes at about 441, 564, and 607 nm, which are redshifted by at least 10 nm compared to those of the unsubstituted lanthanide tetraphenylporphyrinate (TPP) complexes. The large red shifts of both the Soret and Q-bands indicate a decreased energy gap between the HOMO and LUMOs as a consequence of the expanded π-conjugation. This can be attributed to the strong electron-donating ability of the DPA substituents, which produces a profound perturbation of the ground-state properties of the porphyrin TPP.

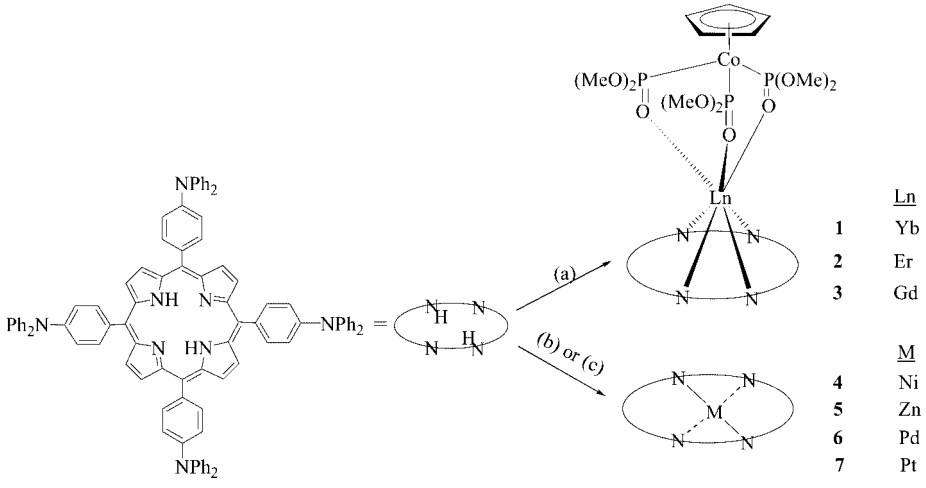

Scheme 1. Synthesis of lanthanide and transition metal monoporphyrinate complexes: (a) Ln[N(SiMe$_3$)$_2$]$_3$·*x*[LiCl(thf)], reflux in toluene, then NaL_{OMe}; (b) M(OAc)$_2$, $CHCl_3$/MeOH (M = Ni, Zn, Pd); (c) [$PtCl_2$(PhCN)$_2$], reflux in PhCN.

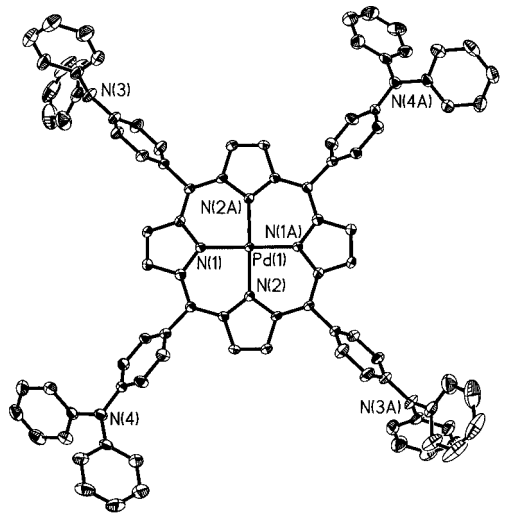

(a)

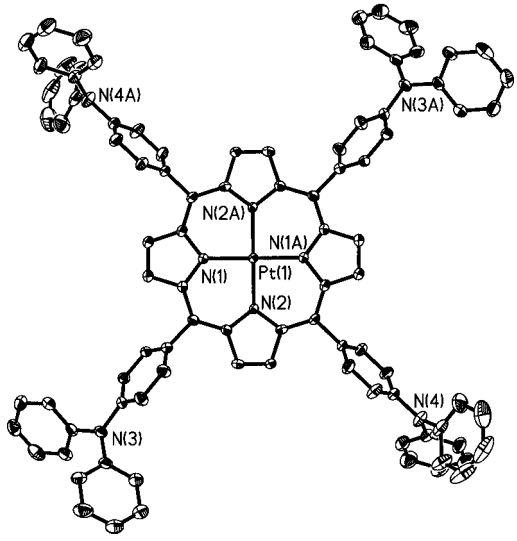

(b)

Figure 1. Perspective views of the crystal structures of **6** (a) and **7** (b). Hydrogen atoms and the labels on all carbon atoms have been omitted for clarity.

Table 1. Selected bond lengths [Å] and angles [°] for **6** and **7**.

	6 [M = Pd]	**7** [M = Pt]
M(1)–N(1)	2.015(3)	2.008(4)
M(1)–N(2)	2.015(3)	2.012(3)
C(5)–C(6)	1.491(5)	1.507(6)
N(3)–C(9)	1.429(5)	1.423(6)
N(3)–C(12)	1.416(6)	1.410(6)
N(3)–C(18)	1.398(6)	1.423(6)
C(28)–C(29)	1.496(5)	1.504(6)
N(4)–C(32)	1.406(5)	1.423(6)
N(4)–C(35)	1.416(5)	1.425(7)
N(4)–C(41)	1.426(5)	1.418(7)
N(1)–M(1)–N(2)	89.89(12)	90.21(14)
C(9)–N(3)–C(12)	120.2(4)	120.8(4)
C(9)–N(3)–C(18)	120.8(4)	121.3(4)
C(32)–N(4)–C(35)	121.1(3)	121.7(5)
C(32)–N(4)–C(41)	121.5(4)	119.6(5)

Optical-Limiting Properties of Lanthanide Monoporphyrinate Complexes

All the samples are stable toward air and laser light under our experimental conditions. In order to characterize the OPL properties at 532 nm excitation, the materials should show weak ground-state absorption at this wavelength. The UV/Vis spectra of the complexes in toluene at room temperature are shown in Figure 2; there is clearly a transparent window at 532 nm for the lanthanide monoporphyrinate complexes.

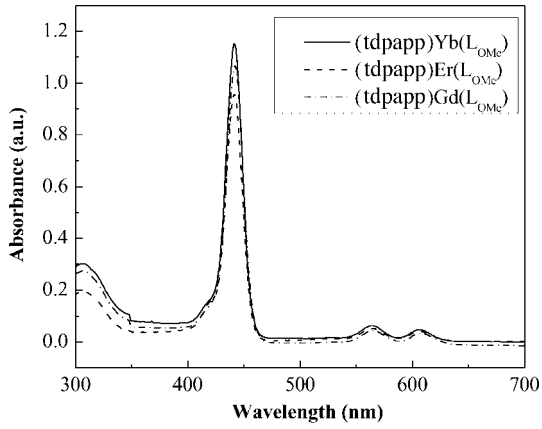

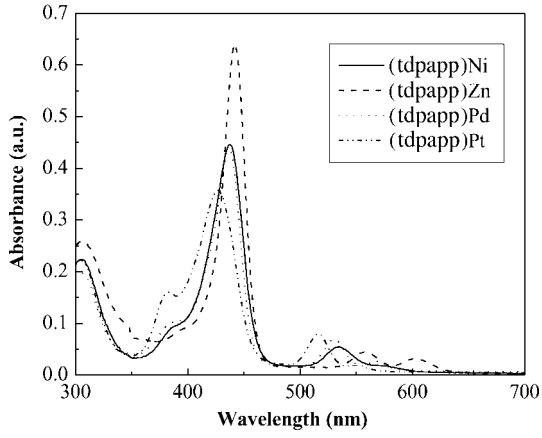

Figure 2. UV/Vis linear-absorption spectra of all the complexes in dilute toluene solution at room temperature.

According to the *Z*-scan curves for all the complexes measured in CH_2Cl_2 (Figure 3), the three lanthanide monoporphyrinate complexes show excellent OPL behavior relative to the benchmark material C_{60}, while the effect is only moderate for the transition metal complexes. Experiments with CH_2Cl_2 alone showed no detectable OPL effect, which indicates that there is a negligible contribution of solvent. When each sample is far from the focus ($Z/Z_0 = 0$) and the incident irradiance upon it is weak, the transmittance of the sample remains almost constant and shows a linear behavior (obeying Beer's law). When the sample is close to the focus, however, and the incident irradiance is strong, the transmittance of the sample decreases rapidly and an OPL

effect appears. It is clear that complex **2** shows the strongest optical-limiting capability, superior even to that of C_{60}, which is generally regarded as an excellent optical limiter. Complexes **1** and **3** also exhibit good OPL properties similar to those of C_{60}. As anticipated, compound **4** with the lighter nickel ion only showed a relatively weaker OPL response among **4**–**7**. On the other hand, we observe that incorporation of DPA units to the porphyrin ring leads to enhanced OPL responses (Figure 4), indicative of strong electronic interaction between the porphyrin and DPA moieties in the present system.

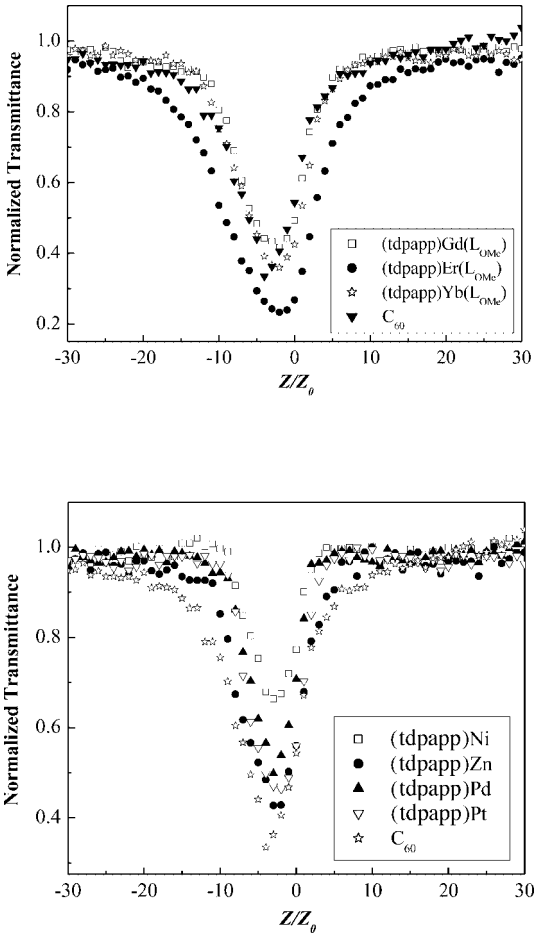

Figure 3. Open-aperture *Z*-scan results for the metal monoporphyrinate complexes and C_{60} solutions at T_o = 82%.

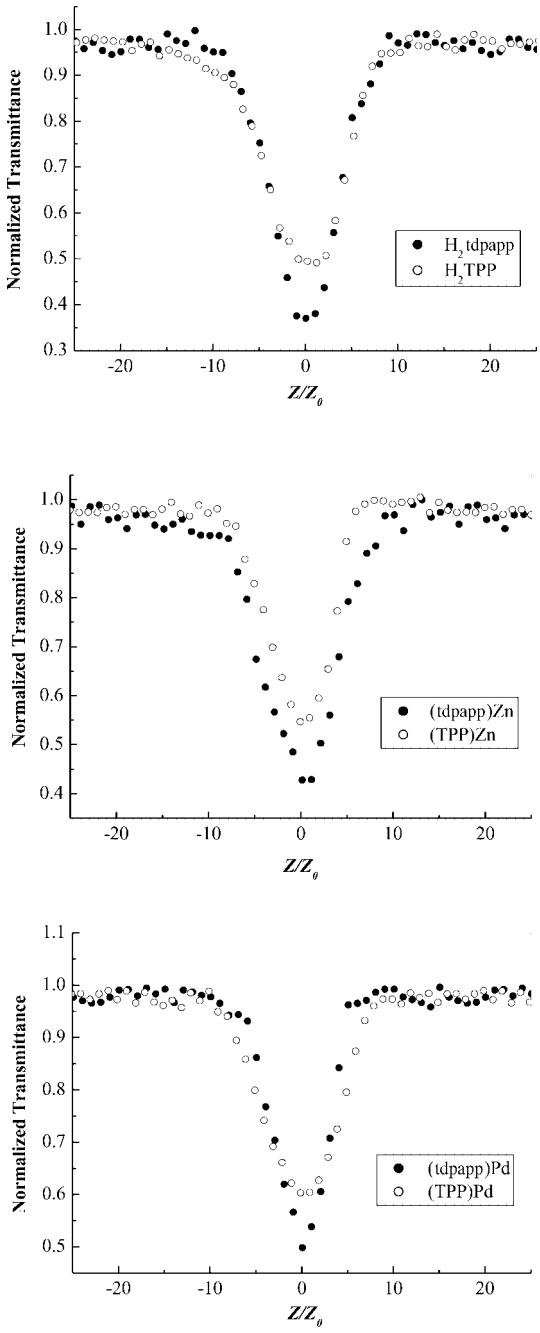

Figure 4. The effect of diphenylamino groups on the open-aperture *Z*-scan results for the free porphyrin and its metal complexes at T_o = 82%.

In order to explain the *Z*-scan data obtained, we must consider the optical-limiting mechanism. According to the five-level model for the RSA mechanism (see Figure 5),[27] the molecules in the ground state (S_0) initially absorb optical energy and are excited to the first singlet state (S_1). After the S_1 state reaches a certain population, it can absorb optical energy strongly and leap to a higher singlet state (S_n), where it can induce an optical-limiting effect or undergo intersystem crossing (ISC) to the first triplet state (T_1). This can then also absorb optical energy strongly to reach a higher triplet state (T_n), which leads to optical-limiting action. Owing to the short lifetime (<10 ns) of the singlet state (see Table 2), it is the triplet-state absorption that contributes to the nanosecond optical-limiting process.[15b,27] To support this, the photoluminescence (PL) spectra for the singlet and triplet states of all complexes were measured (see Figures 6, 7, 8, and 9). At 77 K, the PL spectrum for **3** shows an obvious triplet emission at 815 nm with a measured triplet lifetime of 109 ms. The singlet-state lifetime for **3** is 3.23 ns. Since the pulse lengths are shorter than the lifetime of the triplet state, it acts as an accumulation site. This could confirm that the OPL effect of **3** is mainly induced by the triplet-state absorption. While a more complicated discussion may be invoked for the other

two lanthanide porphyrinate complexes, there is no apparent triplet emission for **1** and **2**, even at 77 K (Figure 6a and b), which suggests that the OPL effects of the Er and Yb complexes are not induced by the triplet-state absorption of the ligands. It is well known that there are efficient energy-transfer processes from the triplet state of the porphyrinate ligand to the excited states of the central lanthanide ions, thus enabling the ion to emit light. The energy absorption that accompanies the transition processes from the lower excited states of the lanthanide ion to the higher energy ones will therefore contribute to the OPL effect of the lanthanide complexes. Owing to the presence of its multiple excited states, the porphyrinate ligand will provide more possible energy absorption transitions in **2** than its Yb counterpart **1**. Complex **2** therefore shows a much better optical-limiting performance than **1**. It can be concluded that the OPL effects of **1** and **2** are predominantly caused by the excited state absorption of the central lanthanide ion. As trivalent lanthanide ions, Yb^{3+} and Er^{3+} should show strong near-infrared (NIR) emission bands.[21a,28] To support this, the NIR PL spectra of **1** and **2** (Figure 7) were measured. Our previous PL studies on related lanthanide porphyrinate complexes have shown that the excitation of Yb^{3+} is due to the $\pi \rightarrow \pi^*$ transitions of the porphyrinate antenna, and that the porphyrinate antenna transfers its absorbed visible energy of the Q-bands to the excited state of the lanthanide ion, which then relaxes through emission in the NIR region.[21a,28b] A strong emission due to the $^2F_{5/2} \rightarrow {}^2F_{7/2}$ transition is observed at 995 nm for the Yb^{3+} complex **1**, whereas for the Er^{3+} complex **2**, the emission at 1529 nm can be assigned to the $^4I_{13/2} \rightarrow {}^4I_{15/2}$ transition. The NIR lifetime of **1** in toluene at room temperature is 30 μs, which also confirms that the excited state of the Yb^{3+} ion should play a major role in the OPL effect of **1**. However, we were unable to measure the NIR lifetime of **2** due to the limitations of the instrument. Unlike **1** and **2**, the OPL effect of **3** should be due to the triplet state of the ligand which can be corroborated by the observation of an obvious triplet emission at 77 K (Figure 6c). Furthermore, the absence of an NIR emission for the Gd^{3+} ion will also preclude the involvement of the excited state of the central Gd ion in the OPL phenomenon. In other words, the OPL effect of **3** is likely dominated by the triplet excited state absorption of the ligand. In view of these factors, complex **3** can be anticipated to show an inferior OPL effect than the free ligand.

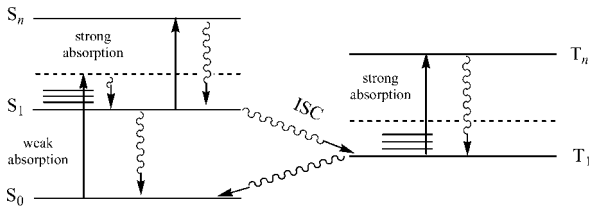

Figure 5. RSA mechanism for the lanthanide monoporphyrinate complexes.

Table 2. Lifetime of the S_1 state for the lanthanide monoporphyrinate complexes.

Complex	Lifetime [ns][a]
[(tdpapp)Yb(L_{OMe})]	1.43
[(tdpapp)Er(L_{OMe})]	3.55
[(tdpapp)Gd(L_{OMe})]	3.23
[Ni(tdpapp)]	< 0.50
[Zn(tdpapp)]	2.66
[Pd(tdpapp)]	1.76
[Pt(tdpapp)]	5.88

[a] Measured at room temperature in toluene solution with an excitation wavelength of 337 nm.

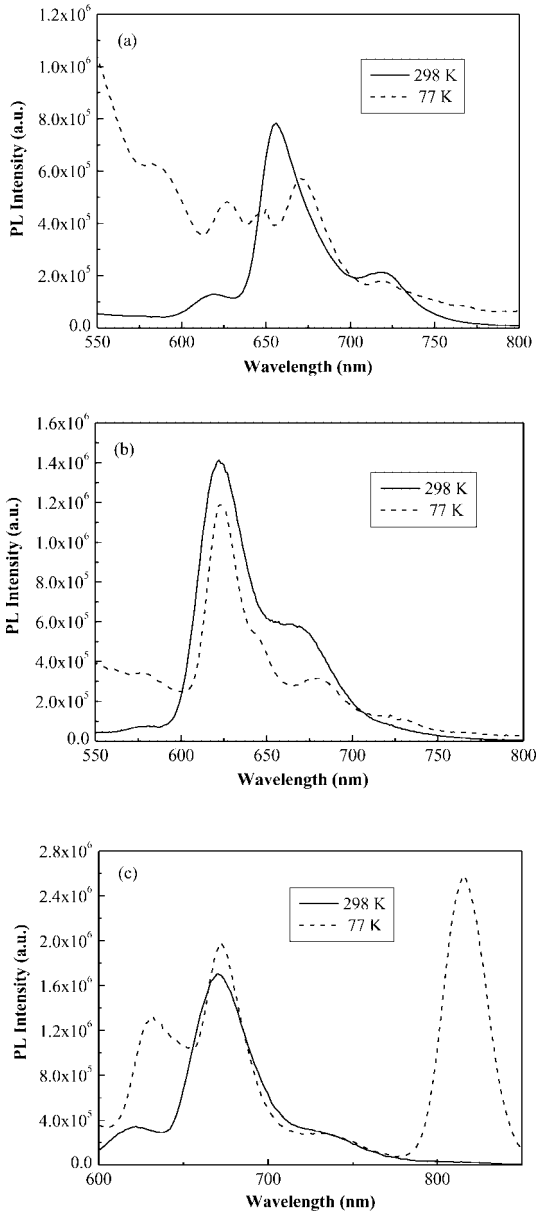

Figure 6. PL spectra for **1** (a), **2** (b), and **3** (c) at 298 and 77 K in toluene.

The OPL effect of H_2tdpapp and **4**–**7** is induced mainly by the strong absorption of the triplet states of the ligand induced by spin-orbital coupling effect, which can be de-

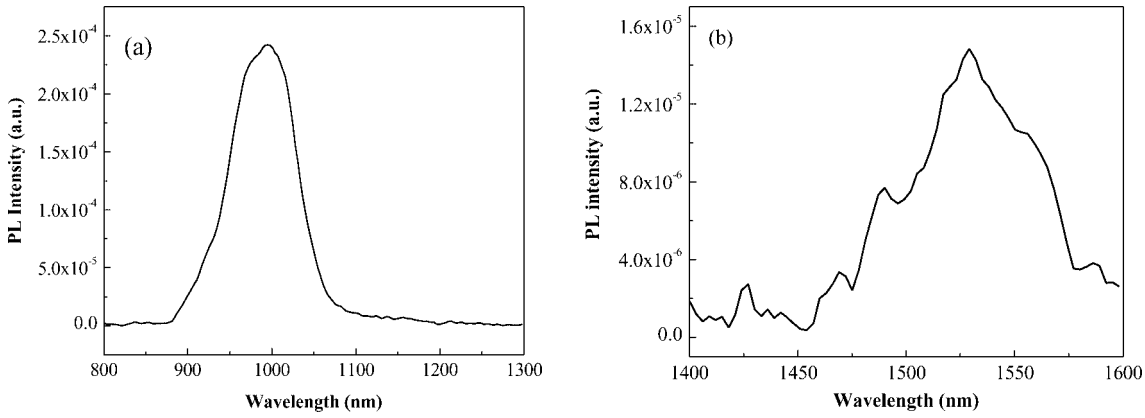

Figure 7. NIR photoluminescence spectra of **1** (a) and **2** (b) in toluene at room temperature.

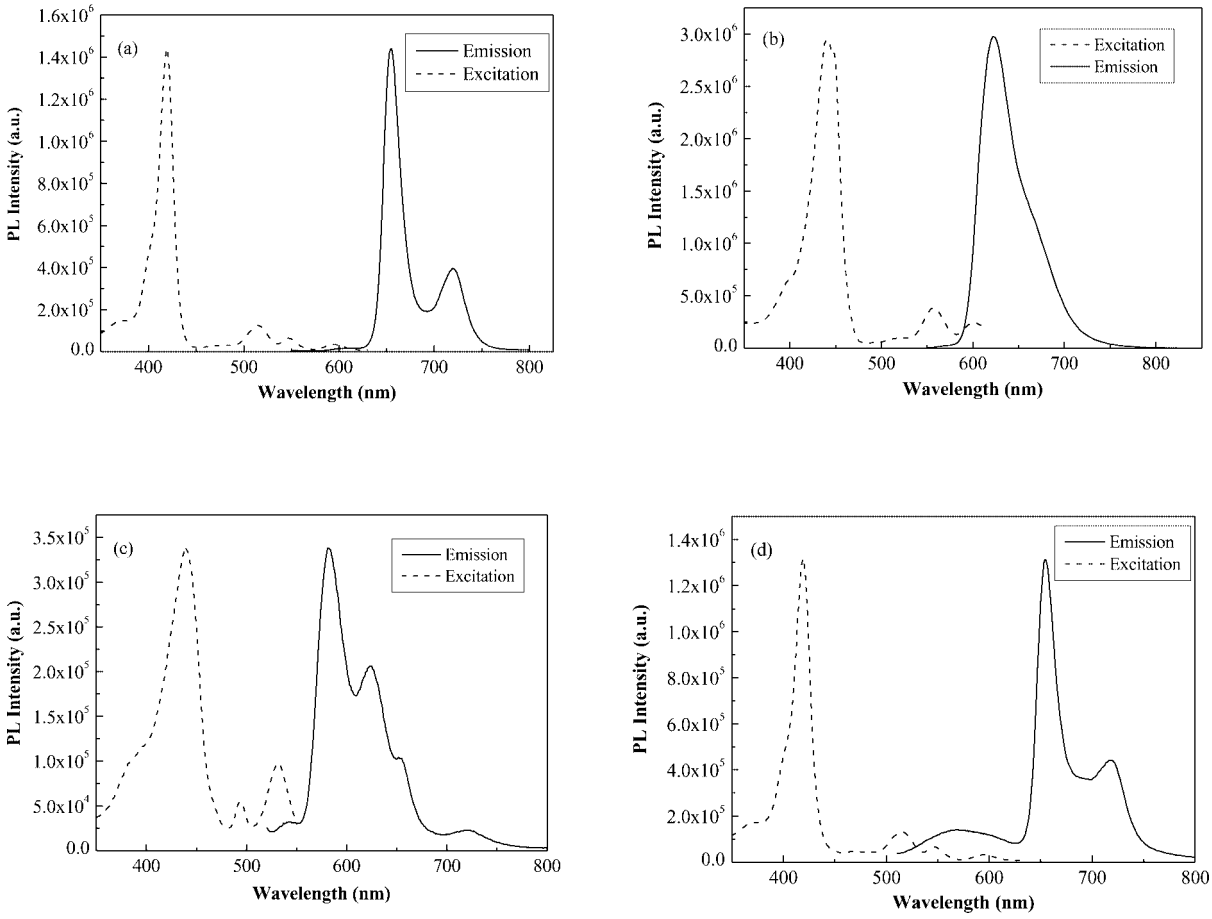

Figure 8. PL spectra for **4** (a), **5** (b), **6** (c), and **7** (d) at 298 K in toluene.

scribed by the typical RSA mechanism (Figure 5) and is typical of other known transition metal porphyrins reported in the literature. The PL spectra of **4**–**7** in toluene at 298 and 77 K are depicted in Figures 8 and 9, respectively. Owing to the much stronger triplet emission at 77 K for **6** (λ_{em} = 723 nm) and **7** (λ_{em} = 689 nm) and their long lifetimes (890 and 80 μs, respectively), both of them show a stronger OPL effect than **4** according to the RSA mechanism stated above. As complex **4** contains the light Ni ion, it is not phosphorescent even at 77 K. The observation of a reasonably strong OPL response for **5**, which also shows no triplet emission at 77 K but only a singlet emission at 630 nm with a lifetime of 7.78 ns at 77 K, can be ascribed to its higher transparency at 532 nm compared with that of other three transition metal complexes (as revealed clearly from the UV/Vis spectra shown in Figure 2). In view of its better transparency, the Zn complex **5** should possess a higher concentration than the others when the OPL signal is measured at the same linear transmittance. As there should be more molecules contributing to its OPL effect,

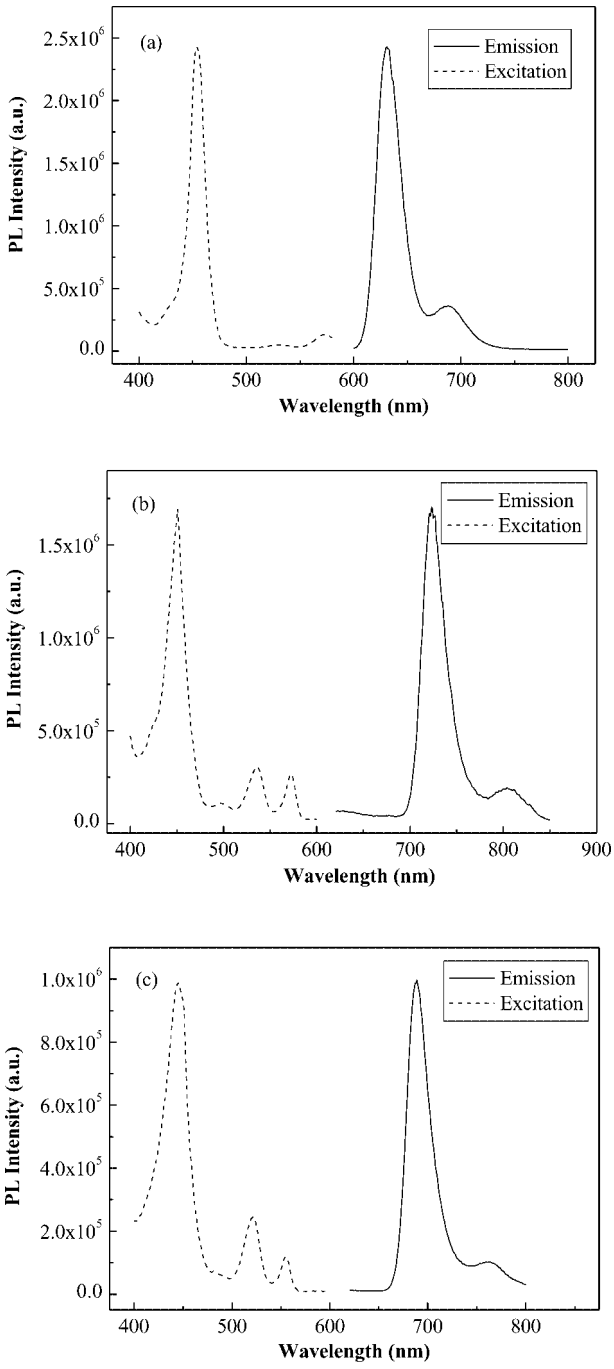

Figure 9. PL spectra for **5** (a), **6** (b), and **7** (c) at 77 K in toluene.

this will compensate for the loss in contribution due to the triplet-state absorption. Hence, despite its low triplet yield, complex **5** can still show an OPL close to those of **6** and **7**.

Figure 10 shows a simple, widely accepted photophysical model of the sensitization process in some (Por)Ln(L_{OMe})-type compounds (Por = porphyrinate anion).[28c,28d,29] In this process, the porphyrin absorbs light and is excited to its singlet state (S_1). The energy is then transferred to its triplet state (T_1), which is, in part, transferred to the excited state of the lanthanide ion (Ln^{3+})* to produce the final luminescence. The Er^{3+} ion is clearly able to introduce more low-lying states in the HOMO–LUMO gap to perturb the ring π-electron system,[16f] which might explain why **2** has the strongest optical-limiting yield of the three lanthanide monoporphyrinate complexes.

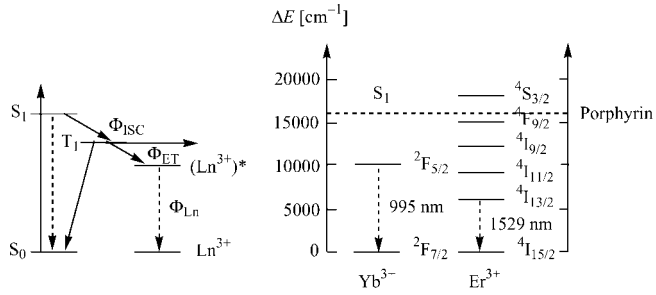

Figure 10. Schematic energy diagram of (Por)Ln(L_{OMe}) complexes. The arrows indicate the excitation mechanism of lanthanide ions by the porphyrin sensitizer ($S_0 \rightarrow S_1$ transition followed by intersystem crossing and energy transfer).

Table 3 lists the optical-limiting thresholds of the three lanthanide monoporphyrinate complexes, which is an important parameter in characterizing the merit of these optical limiters. All three complexes possess low optical-limiting thresholds at 82% linear transmittance. Complex **2** shows a lower optical-limiting threshold than fullerene C_{60} that is even comparable to those of some state-of-the-art phthalocyanine dyes. The optical-limiting thresholds of the transition metal analogues **4**–**7** are, however, less attractive than the lanthanide congeners. Hence, the OPL effects of the functionalized porphyrin H_2tdpapp can be enhanced greatly by the incorporation of trivalent lanthanide ions.

Concluding Remarks

We have reported a series of new lanthanide monoporphyrinate complexes that exhibit excellent optical-limiting capabilities for a nanosecond laser pulse at 532 nm and display optical-limiting thresholds comparable to or lower than those reported for optical-limiting materials currently in use. Experimental investigations on their photophysics suggest that these complexes show optical-limiting effects following the standard five-level RSA mechanism. The optical-limiting effects of porphyrins can be enhanced greatly by the addition of electron-rich Ph_2N groups and the incorporation of lanthanide ions, which can make the energy of the porphyrin triplet state transfer efficiently to the excited state of the lanthanide ions. We have shown that the three monoporphyrinate lanthanide complexes have an excellent optical-limiting performance and are very promising candidates for practical use as optical-limiting materials for the protection of optical devices. Solid films are desirable for many optical power-limiting applications, therefore further work will be carried out to determine the response of polymer films to an optical pulse for use in practical devices.

Table 3. Comparison of the optical-limiting performance of **1**–**7** with some reported materials.

Compound	Optical limiting threshold [J cm^{-2}][b]	T_o [%][c]	Sample thickness [mm]	σ_{ex}/σ_o[a]	Reference
PbPc(β-CP)$_4$	0.070	62	[d]	[d]	[30]
CuPcR$_8$[e]	0.30	68	10	4.18	[31]
MPc; M = Si, Ge, etc	0.10	84	10	[d]	[32]
C_{60}	0.18	55	2	[d]	[33]
C_{60}	0.19	84	1	5.74	this work
H_2tdpapp	0.27	82	1	5.35	this work
[(tdpapp)Yb(L_{OMe})]	0.17	82	1	5.42	this work
[(tdpapp)Er(L_{OMe})]	0.093	82	1	7.35	this work
[(tdpapp)Gd(L_{OMe})]	0.30	82	1	4.80	this work
[Ni(tdpapp)]	1.99[f]	82	1	2.67	this work
[Zn(tdpapp)]	0.38	82	1	4.69	this work
[Pd(tdpapp)]	0.69	82	1	3.95	this work
[Pt(tdpapp)]	0.46	82	1	4.39	this work

[a] $\sigma_{ex}/\sigma_o = \ln T_{sat}/\ln T_o$, where σ_{ex} is the effective excited-state absorption cross-section, σ_o is the ground-state absorption cross-section, and T_{sat} is the transmittance at the saturation fluence. [b] The optical-limiting threshold is defined as the input light fluence at which the output light fluence is 50% of that predicted by linear transmittance. [c] Linear transmittance. [d] Not reported. [e] R = pentyloxy. [f] Predicted by theoretical fitting.

Experimental Section

General: All reactions were carried out under dry nitrogen. Solvents were dried by standard procedures, distilled, and degassed prior to use. All chemicals used were purchased from Aldrich or Acros. 4-(Diphenylamino)benzaldehyde was prepared according to a literature method by formylation of triphenylamine with dmf and $POCl_3$.[34] 5,10,15,20-Tetrakis[*p*-(diphenylamino)phenyl]-21*H*,23*H*-porphine (H_2tdpapp) was also prepared according to a literature method by condensing pyrrole and 4-(diphenylamino)benzaldehyde.[24] NMR spectra were measured in $CDCl_3$ with a JEOL EX270 or a Varian Inova 400 MHz FT-NMR spectrometer, with the ^{1}H NMR chemical shifts quoted relative to $SiMe_4$ and the ^{31}P NMR chemical shifts relative to 85% H_3PO_4 as external standard. Electrospray ionization high-resolution mass spectra were recorded with a QSTAR mass spectrometer. The electronic absorption spectra in the UV/Vis region were obtained with a Hewlett Packard 8453 spectrophotometer. The photoluminescent properties and lifetimes of the complexes were determined with a Photon Technology International (PTI) spectrophotometer. NIR emission was detected by a liquid-nitrogen-cooled InSb IR detector (EG & G) with a preamplifier, and recorded by a lock-in amplifier system. The third harmonic of the 355-nm line of an Nd:YAG laser (Quantel Brilliant B) was used as the excitation light source. Infrared spectra were obtained with a Nicolet Magna 550 series II FTIR spectrometer in KBr pellets.

Optical-Limiting Measurements: To study the optical-limiting properties, intensity-dependent transmittance and *Z*-scan measurements were performed with a Q-switched Nd:YAG laser at a repetition rate of 10 Hz. The laser frequency was doubled with an output wavelength of 532 nm and a 10-ns pulse width for the Gaussian mode by a frequency double crystal. The laser beam was then split into two by a beam splitter. One was used as the reference beam, which was received by a detector (D_1), and the other was used for the sample measurement, and was focused with a lens (f = 20 cm). After transmitting through the sample, the light beam entered another detector (D_2). The sample to be measured was moved along a rail to change the incident irradiance on it. The incident and transmitted energies were detected simultaneously by the two detectors D_1 and D_2 (LPE-1A). The performance of each sample was measured as an 82% transmitting solution at 532 nm in CH_2Cl_2 in a 1-mm quartz cell.

Preparation of Precursor Complexes: Stock solutions of the precursor complexes, Ln[N(SiMe$_3$)$_2$]$_3$·*x*[LiCl(thf)$_3$] (Ln = Yb^{3+}, Er^{3+} and Gd^{3+}), were prepared in a similar manner. A detailed description is given for the Yb^{3+} complex.

Yb[N(SiMe$_3$)$_2$]$_3$·*x*[LiCl(thf)$_3$] (Solution A): HN(SiMe$_3$)$_2$ (5.06 mL, 0.024 mol) was dissolved in thf (10 mL) in an ice bath, then *n*BuLi (1.6 M in hexane; 15.0 mL, 0.024 mol) was added slowly over a period of 30 min. The resulting solution was magnetically stirred for 12 h until a clear pale yellow solution was obtained. The solution was then transferred slowly into a Schlenk flask containing $YbCl_3$ (2.24 g, 0.008 mol) suspended in thf (20 mL). The resulting mixture was magnetically stirred for 24 h until all of the solid $YbCl_3$ had disappeared. The resulting solution A contains Yb[N(SiMe$_3$)$_2$]$_3$·*x*[LiCl(thf)] (*x* = 3–5).

Er[N(SiMe$_3$)$_2$]$_3$·*x*[LiCl(thf)$_3$] (Solution B): Er[N(SiMe$_3$)$_2$]$_3$·*x*[LiCl(thf)$_3$] was prepared by the same method as for solution A except that HN(SiMe$_3$)$_2$ (5.06 mL, 0.024 mol), *n*BuLi (1.6 M in hexane; 15.0 mL, 0.024 mol), and $ErCl_3$ (2.18 g, 0.008 mol) in thf were used.

Gd[N(SiMe$_3$)$_2$]$_3$·*x*[LiCl(thf)$_3$] (Solution C): Gd[N(SiMe$_3$)$_2$]$_3$·*x*[LiCl(thf)$_3$] was prepared similarly as for solution A except that HN(SiMe$_3$)$_2$ (5.06 mL, 0.024 mol), *n*BuLi (1.6 M in hexane; 15.0 mL, 0.024 mol), and $GdCl_3$ (2.11 g, 0.008 mol) in thf were used.

Synthesis of Complexes 1–3: Compounds **1**–**3** were prepared according to the same procedure. A typical procedure is given for **1**. We used the tripodal anion L_{OMe}^- {L_{OMe}^- = (η^5-C_5H_5)Co[P(=O)(OMe)$_2$]$_3^-$} to stabilize labile normal lanthanide(III) porphyrinate complexes.

[(tdpapp)Yb(L_{OMe})] (1): Solution A (2.0 mL, 0.32 mmol) was transferred into a Schlenk flask and the solvent was removed under vacuum. Dichloromethane (10 mL) was then added to precipitate LiCl. The mixture was centrifuged and the clear layer was transferred to another Schlenk flask containing dry H_2tdpapp (50 mg, 0.039 mmol) dissolved in toluene (15 mL). The progress of the reaction was monitored by UV/Vis spectroscopy. The resulting solution was refluxed for 12 h until most of the free base had coordinated to the metal ion. Upon cooling of the reaction mixture to room temperature, solid NaL_{OMe} (0.1 g, 0.22 mmol) was added and the resultant solution was magnetically stirred for another 24 h. The

solvent was removed in vacuo, and the residue was dissolved in chloroform, filtered, and chromatographed on silica gel using chloroform/petroleum ether (1:1, v/v) as the eluent. Complex **1** was obtained in 75% yield (56 mg). IR (KBr): $\tilde{\nu}$ = 3445 m, 2940 m, 1591 s, 1490 s, 1276 m, 1143 s, 1006 m, 752 m, 696 m cm^{-1}. ^{1}H NMR ($CDCl_3$): δ = 16.39 (s, 4 H, Ar), 15.57 (s, 8 H, β-H), 10.30 (s, 4 H, Ar), 8.58–8.56 (m, 24 H, Ar), 8.11–8.07 (m, 16 H, Ar), 7.63–7.61 (m, 8 H, Ar), 6.44 (s, 18 H, OMe), –4.71 (s, 5 H, η^5-C_5H_5) ppm. ^{31}P NMR ($CDCl_3$): δ = 68.29 (s) ppm. UV/Vis (toluene, 20 °C): λ_{max} (logε) = 307 (5.18), 441 (5.76), 564 (4.50), 607 (4.38 M^{-1}cm^{-1}) nm. ESI-HRMS ($CHCl_3$): *m*/*z* = 1906.4548 [M + H]$^+$.

[(tdpapp)Er(L_{OMe})] (2): Solution B (2.0 mL, 0.32 mmol), H_2tdpapp (100 mg, 0.078 mmol), and NaL_{OMe} (0.1 g, 0.22 mmol) were used. Yield: 81% (120 mg). IR (KBr): $\tilde{\nu}$ = 3445 m, 2940 m, 1591 s, 1490 s, 1277 s, 1141 s, 1006 s, 796 m, 752 m, 696 m cm^{-1}. ^{1}H NMR ($CDCl_3$): δ = 45.59 (s, 4 H, Ar), 35.09 (s, 8 H, β-H), 20.64–19.99 (m, 24 H, Ar), 12.56 (s, 18 H, OMe), 12.14 (s, 4 H, Ar), 10.39 (s, 16H, Ar), 9.43 (s, 8 H, Ar), –34.16 (s, 5 H, η^5-C_5H_5) ppm. ^{31}P NMR ($CDCl_3$): δ = –166.01 (s) ppm. UV/Vis (toluene, 20 °C): λ_{max} (logε) = 307 (4.99), 441 (5.68), 564 (4.41), 606 (4.31 M^{-1}cm^{-1}) nm. ESI-HRMS ($CHCl_3$): *m*/*z* = 1899.4461 [M]$^+$.

[(tdpapp)Gd(L_{OMe})] (3): Solution C (2.0 mL, 0.32 mmol), H_2tdpapp (100 mg, 0.078 mmol), and NaL_{OMe} (0.1 g, 0.22 mmol) were used. Yield: 76% (112 mg). IR (KBr): $\tilde{\nu}$ = 3449 m, 2940 m, 1591 s, 1491 s, 1277 m, 1137 s, 1006 m, 752 m, 696 m cm^{-1}. UV/Vis (toluene, 20 °C): λ_{max} (logε) = 307 (5.14), 442 (5.73), 566 (4.35), 608 (4.24 M^{-1}cm^{-1}) nm. ESI-HRMS ($CHCl_3$): *m*/*z* = 1890.4455 [M + H]$^+$.

Synthesis of Complexes 4–7: Transition metal porphyrinate complexes **4**–**7** were prepared by refluxing the porphyrin free-base with 1 equiv. of the metal salts in an appropriate solvent. The typical procedure is described in detail for **4**.

[Ni(tdpapp)] (4): $Ni(OAc)_2$·$4H_2O$ (100 mg, 0.4 mmol) dissolved in MeOH (8 mL) was added to a solution of H_2tdpapp (50 mg, 0.039 mmol) in $CHCl_3$ (30 mL). The mixture was then refluxed until the reaction was complete, as revealed by TLC. The product was purified on silica gel using chloroform/petroleum ether (2:1, v/v) as the eluent. The title product was obtained in 92% yield (48 mg). IR (KBr): $\tilde{\nu}$ = 3444 m, 3029 w, 1591 s, 1491 s, 1280 s, 1177 w, 1002 m, 800 m, 753 m, 695 m cm^{-1}. ^{1}H NMR ($CDCl_3$): δ = 8.81 (s, 8 H, β-H), 7.78 (d, *J* = 8.4 Hz, 8 H, Ar), 7.34–7.28 (m, 40 H, Ar), 7.06–7.01 (m, 8 H, Ar) ppm. UV/Vis (toluene, 20 °C): λ_{max} (logε) = 304 (5.05), 437 (5.35), 534 (4.44 M^{-1}cm^{-1}) nm. ESI-HRMS ($CHCl_3$): *m*/*z* = 1339.4674 [M]$^+$.

[Zn(tdpapp)] (5): H_2tdpapp (50 mg, 0.039 mmol) and $Zn(OAc)_2$·$2H_2O$ (50 mg, 0.23 mmol) were used. Yield: 96% (50 mg). IR (KBr): $\tilde{\nu}$ = 3446 m, 3027 w, 1590 s, 1489 s, 1279 s, 1176 w, 999 m, 798 m, 753 m, 695 m cm^{-1}. ^{1}H NMR ($CDCl_3$): δ = 9.03 (s, 8 H, β-H), 8.01 (d, *J* = 8.4 Hz, 8 H, Ar), 7.40–7.33 (m, 40 H, Ar), 7.07–7.04 (m, 8 H, Ar) ppm. UV/Vis (toluene, 20 °C): λ_{max} (logε) = 306 (5.11), 442 (5.51), 558 (4.35), 603 (4.20 M^{-1}cm^{-1}) nm. ESI-HRMS ($CHCl_3$): *m*/*z* = 1346.4536 [M]$^+$.

[Pd(tdpapp)] (6): H_2tdpapp (50 mg, 0.039 mmol) and $Pd(OAc)_2$ (50 mg, 0.22 mmol) were used. Yield: 89% (48 mg). IR (KBr): $\tilde{\nu}$ = 3443 m, 3029 w, 1591 s, 1491 s, 1278 s, 1175 w, 1014 m, 805 w, 751 m, 695 m cm^{-1}. ^{1}H NMR ($CDCl_3$): δ = 8.90 (s, 8 H, β-H), 7.96 (d, *J* = 8.4 Hz, 8 H, Ar), 7.39–7.33 (m, 40 H, Ar), 7.09–7.07 (m, 8 H, Ar) ppm. UV/Vis (toluene, 20 °C): λ_{max} (logε) = 307 (4.99), 437 (5.34), 530 (4.54), 569 (4.13 M^{-1}cm^{-1}) nm. ESI-HRMS ($CHCl_3$): *m*/*z* = 1386.4327 [M]$^+$.

[Pt(tdpapp)] (7): A solution of H_2tdpapp (100 mg, 0.078 mmol) and $PtCl_2(PhCN)_2$ (74 mg, 0.156 mmol) in benzonitrile (10 mL) was heated at reflux to afford **7** in 87% yield (100 mg).[35] IR (KBr): $\tilde{\nu}$ = 3444 m, 3029 w, 1591 s, 1491 s, 1281 s, 1177 w, 1021 m, 803 w, 753 m, 695 m cm^{-1}. ^{1}H NMR ($CDCl_3$): δ = 8.85 (s, 8 H, β-H), 7.93 (d, *J* = 8.1 Hz, 8 H, Ar), 7.38–7.33 (m, 40 H, Ar), 7.08–7.06 (m, 8 H, Ar) ppm. UV/Vis (toluene, 20 °C): λ_{max} (logε) = 305 (5.16), 428 (5.25), 516 (4.58), 551 (3.94 M^{-1}cm^{-1}) nm. ESI-HRMS ($CHCl_3$): *m*/*z* = 1476.4990 [M]$^+$.

X-ray Crystallography: Crystals of **6**·$2CHCl_3$ and **7**·$2CHCl_3$ suitable for X-ray diffraction were grown by slow concentration of chloroform solutions of these compounds in air. Because of severe solvent loss, the selected crystals were mounted in sealed capillary tubes for diffraction experiments. The intensity data were collected at 293 K with a Bruker AXS SMART 1000 CCD area-detector diffractometer using graphite-monochromated Mo-K_α radiation (λ = 0.71073 Å). The collected frames were processed with proprietary software (SAINT[36]) and an absorption correction was applied (SADABS[37]) to the collected reflections. The structures of these molecules were solved by direct methods and expanded by standard difference Fourier syntheses using the software SHELXTL.[38] Structure refinements were made on F^2 using the full-matrix least-squares technique. All non-hydrogen atoms were refined with anisotropic displacement parameters. Hydrogen atoms were placed in their idealized positions and allowed to ride on the respective carbon atoms. Pertinent crystallographic data and other experimental details are summarized in Table 4. CCDC-628463 (**6**) and -628464 (**7**) contain the supplementary crystallographic data for this paper. These data can be obtained free of charge from The Cambridge Crystallographic Data Centre via www.ccdc.cam.ac.uk/data_request/cif.

Table 4. Crystal data and refinement for compounds **6** and **7**.

	6·$2CHCl_3$	**7**·$2CHCl_3$
Empirical formula	$C_{94}H_{66}N_8Cl_6Pd$	$C_{94}H_{66}N_8Cl_6Pt$
Formula mass	1626.65	1715.34
Crystal system	monoclinic	monoclinic
Space group	$P2_1/n$	$P2_1/n$
a [Å]	17.4493(10)	17.441(2)
b [Å]	9.4600(6)	9.4752(12)
c [Å]	24.3486(14)	24.345(3)
β [°]	104.8050(10)	104.778(2)
V [Å^3]	3885.8(4)	3890.2(9)
Z	2	2
F(000)	1668	1732
$D_{calcd.}$ [g cm^{-3}]	1.390	1.464
μ(Mo-K_α) [mm^{-1}]	0.500	2.064
Reflections collected	18533	18744
Unique reflections	6800	6810
Observed reflections	4139	4462
GOF on F^2	1.009	1.056
R_1, wR_2 [$I > 2\sigma(I)$]	0.0657, 0.1718	0.0436, 0.1145
R_1, wR_2 (all data)	0.1174, 0.2082	0.0776, 0.1304

Acknowledgments

We thank the Hong Kong Baptist University (FRG/03-04/II-52) and Hong Kong Research Grants Council (HKBU 2021/03P) for their financial support.

[1] L. W. Tutt, T. F. Boggess, *Prog. Quantum Electron.* **1993**, *17*, 299.
[2] D. G. Mclean, R. L. Sutherland, M. C. Brant, D. M. Brandelick, P. A. Fleitz, T. Potten, *Opt. Lett.* **1993**, *18*, 858.

[3] W. Blau, H. Byrne, W. M. Dennis, J. M. Kelly, *Opt. Commun.* **1985**, *56*, 25.
[4] G. De La Torre, P. Vázquez, F. Agulló-López, T. Torres, *J. Mater. Chem.* **1998**, *8*, 1671.
[5] G. L. Wood, M. J. Miller, A. G. Mott, *Opt. Lett.* **1995**, *20*, 973.
[6] A. Krivokapic, H. L. Anderson, G. Bourhill, R. Ives, S. Clark, K. J. McEwan, *Adv. Mater.* **2001**, *13*, 652.
[7] M. Cha, N. S. Sariciftci, A. J. Hegger, J. C. Hummelen, F. Wudl, *Appl. Phys. Lett.* **1995**, *67*, 3850.
[8] L. C. Song, G. A. Yu, H. T. Wang, F. H. Su, Q. M. Hu, Y. L. Song, Y. C. Gao, *Eur. J. Inorg. Chem.* **2004**, 866.
[9] N. V. Kamanina, I. Y. Denisyuk, *Opt. Spectrosk.* **2004**, *96*, 77.
[10] Y. Chen, S. O'Flaherty, M. Fujitsuka, M. Hanack, L. R. Subramanian, O. Ito, W. J. Blau, *Chem. Mater.* **2002**, *14*, 5163.
[11] P. Zhu, C. Yu, J. Liu, Y. Song, C. Li, *Proc. SPIE-Int. Soc. Opt. Eng.* **1996**, *2879*, 289.
[12] K. P. Loh, H. Zhang, W. Z. Chen, W. Ji, *J. Phys. Chem. B* **2006**, *110*, 1235.
[13] M. Pittman, P. Plaza, M. M. Martin, Y. H. Meyer, *Opt. Commun.* **1998**, *158*, 201.
[14] A. Baev, O. Rubio-Pons, F. Gel'mukhanov, H. Ågren, *J. Phys. Chem. A* **2004**, *108*, 7406.
[15] a) G.-J. Zhou, S. Zhang, P.-J. Wu, C. Ye, *Chem. Phys. Lett.* **2002**, *363*, 610; b) G.-J. Zhou, W.-Y. Wong, D. M. Cui, C. Ye, *Chem. Mater.* **2005**, *17*, 5209; c) G.-J. Zhou, W.-Y. Wong, Z. Lin, C. Ye, *Angew. Chem. Int. Ed.* **2006**, *45*, 6189.
[16] a) K. Sendhil, C. Vijayan, M. P. Kothiyal, *Opt. Mater.* **2005**, *27*, 1606; b) X. H. Zhong, Y. Y. Feng, S. L. Ong, J. Y. Hu, W. J. Ng, Z. M. Wang, *Chem. Commun.* **2003**, *15*, 1882; c) G. Y. Yang, S. G. Ang, L. L. Chng, Y. W. Lee, W. P. Lau, K. S. Lai, H. G. Ang, *Chem. Eur. J.* **2003**, *9*, 900; d) K. J. McEwan, G. Bourhill, J. M. Robertson, H. L. Anderson, *J. Nonlinear Opt. Phys. Mater.* **2000**, *9*, 451; e) B. Dupuis, C. Michaut, I. Jouanin, J. Delaire, P. Robin, P. Feneyrou, V. Dentan, *Chem. Phys. Lett.* **1999**, *300*, 169; f) K. Kandasamy, S. J. Shetty, P. N. Puntambekar, T. S. Srivastava, T. Kundu, B. P. Singh, *J. Porphyrins Phthalocyanines* **1999**, *3*, 81.
[17] a) P. P. Kiran, D. R. Reddy, B. G. Maiya, A. K. Dharmadhikari, G. R. Kumar, N. R. Desai, *Appl. Opt.* **2002**, *41*, 7631; b) K. P. Prem, R. D. Raghunath, B. G. Maiya, R. D. Narayana, *Opt. Mater.* **2003**, *21*, 565.
[18] R. B. Martin, H. P. Li, L. R. Gu, S. Kumar, C. M. Sanders, Y. P. Sun, *Opt. Mater.* **2005**, *27*, 1340.
[19] a) D. Y. Wang, W. F. Sun, S. M. Dong, J. H. Si, C. F. Li, *Mater. Res. Soc. Symp. Proc.* **1997**, *479*, 41; b) W. F. Sun, C. C. Byeon, C. M. Lawson, G. M. Gray, D. Y. Wang, *Appl. Phys. Lett.* **1999**, *74*, 3254; c) D. Y. Wang, W. F. Sun, C. F. Wang, F. Q. Guo, Y. H. Zou, *Proc. SPIE-Int. Soc. Opt. Eng.* **1998**, *3472*, 53.
[20] R. T. Kuznetsova, T. N. Kopylova, G. V. Mayer, L. G. Samsonova, V. A. Svetlichnyi, A. V. Vasil'ev, D. N. Filinov, E. N. Tel'minov, N. S. Kabotaeva, N. V. Svarovskaya, V. M. Podgaetskii, A. V. Reznichenko, *Quantum Electron.* **2004**, *34*, 139.
[21] a) H.-S. He, J.-P. Guo, Z.-X. Zhao, W.-K. Wong, W.-Y. Wong, W.-K. Lo, K.-F. Li, L. Luo, K.-W. Cheah, *Eur. J. Inorg. Chem.* **2004**, 837; b) M. P. Oude Wolebers, F. C. J. M. Van Veggel, B. H. M. Snellink-Ruel, J. W. Hofstraat, F. A. J. Geurts, D. N. Reinhoudt, *J. Chem. Soc., Perkin Trans. 2* **1998**, 2141.
[22] a) P. Strohriegl, J. V. Grazulevicius, *Adv. Mater.* **2002**, *14*, 1439; b) R. D. Hreha, C. P. George, A. Haldi, B. Domercq, M. Malagoli, S. Barlow, J.-L. Brédas, B. Kippelen, S. R. Marder, *Adv. Funct. Mater.* **2003**, *13*, 967; c) P. Kunda, K. R. Justin Thomas, J. T. Lin, Y.-T. Tao, C.-H. Chien, *Adv. Funct. Mater.* **2003**, *13*, 445; d) L. A. Majewski, R. Schroeder, M. Grell, *Adv. Funct. Mater.* **2005**, *15*, 1017; e) N. Satoh, T. Nakashima, K. Yamamoto, *J. Am. Chem. Soc.* **2005**, *127*, 13030; f) W.-Y. Wong, G.-J. Zhou, X.-M. Yu, H.-S. Kwok, B.-Z. Tang, *Adv. Funct. Mater.* **2006**, *16*, 838; g) X.-M. Yu, H.-S. Kwok, W.-Y. Wong, G.-J. Zhou, *Chem. Mater.* **2006**, *18*, 5097.
[23] a) B. Li, X. Xu, M. Sun, Y. Fu, G. Yu, Y. Liu, Z. Bo, *Macromolecules* **2006**, *39*, 456; b) M. J. Frampton, R. Beavington, J. M. Lupton, I. D. W. Samuel, P. L. Burn, *Synth. Met.* **2001**, *121*, 1671; c) J.-C. Chang, C.-J. Ma, G.-H. Lee, S.-M. Peng, C.-Y. Yeh, *Dalton Trans.* **2005**, 1504; d) T.-G. Zhang, Y. Zhao, K. Song, I. Asselberghs, A. Persoons, K. Clays, M. J. Therien, *Inorg. Chem.* **2006**, *45*, 9703.
[24] C. W. Huang, K. Y. Chiu, S. H. Cheng, *Dalton Trans.* **2005**, 2417.
[25] W.-N. Yen, S.-S. Lo, M.-C. Kuo, C.-L. Mai, G.-H. Lee, S.-M. Peng, C.-Y. Yeh, *Org. Lett.* **2006**, *8*, 4239.
[26] a) C. K. Schauer, O. P. Anderson, S. S. Eaton, G. R. Eaton, *Inorg. Chem.* **1985**, *24*, 4082; b) W. R. Scheidt, M. E. Kastner, K. Hatano, *Inorg. Chem.* **1978**, *17*, 706.
[27] S. V. Rao, D. N. Rao, J. A. Akkara, B. S. DeCristifano, D. V. G. L. N. Rao, *Chem. Phys. Lett.* **1998**, *297*, 491.
[28] a) A. Beeby, R. S. Dickins, S. Faulkner, D. Parker, J. A. G. Williams, *Chem. Commun.* **1997**, 1401; b) W.-K. Wong, A.-X. Hou, J.-P. Guo, H.-S. He, L.-L. Zhang, W.-Y. Wong, K.-F. Li, K.-W. Cheah, F. Xue, T. C.-W. Mak, *J. Chem. Soc., Dalton Trans.* **2001**, 3092; c) W. D. Horrocks Jr, J. P. Bolender, W. D. Smith, R. M. Supkowski, *J. Am. Chem. Soc.* **1997**, *119*, 5972; d) G. A. Hebbink, L. Grave, L. A. Woldering, D. N. Reinhoudt, F. C. J. M. Van Veggel, *J. Phys. Chem. A* **2003**, *107*, 2483.
[29] a) M. H. V. Werts, J. W. Hofstraat, F. A. J. Geurts, J. W. Verhoeven, *Chem. Phys. Lett.* **1997**, *276*, 196; b) G. F. De Sá, O. L. Malta, C. De Mello Donegá, A. M. Simas, R. L. Longo, P. A. Santa-Cruz, E. F. Da Silva Jr, *Coord. Chem. Rev.* **2000**, *196*, 165; c) F. R. G. Silva, O. L. Malta, C. Reinhard, H. U. Güdel, C. Piguet, J. E. Moser, J. C. G. Bünzli, *J. Phys. Chem. A* **2002**, *106*, 1670.
[30] J. S. Shirk, R. G. S. Pong, S. R. Flom, F. J. Bartoli, M. E. Boyle, A. W. Snow, *Pure Appl. Opt.* **1996**, *5*, 701.
[31] T. C. Wen, I. D. Lian, *Synth. Met.* **1996**, *83*, 111.
[32] J. W. Perry, K. Mansour, S. R. Marder, K. J. Perry, D. Alvarez Jr, I. Choong, *Opt. Lett.* **1994**, *19*, 625.
[33] Y. P. Sun, J. E. Riggs, B. Liu, *Chem. Mater.* **1997**, *9*, 1268.
[34] J. Ostrauskaite, V. Voska, J. Antulis, V. Gaidelis, V. Jankauskas, J. V. Glazulevicius, *J. Mater. Chem.* **2002**, *12*, 3469.
[35] S. W. Lai, Y. J. Hou, C. M. Che, H. L. Pang, K. Y. Wong, C. K. Chang, N. Y. Zhu, *Inorg. Chem.* **2004**, *43*, 3724.
[36] *SAINT+*, ver. 6.02a, Bruker Analytical X-ray System, Inc., Madison, WI, **1998**.
[37] G. M. Sheldrick, *SADABS, Empirical Absorption Correction Program*, University of Göttingen, Germany, **1997**.
[38] G. M. Sheldrick, *SHELXTL™, Reference manual*, ver. 5.1, Madison, WI, **199**.

Received: December 15, 2006
Published Online: April 4, 2007

